Thin Films and Coatings

MS.5.P125
The Influence of the Electron Beam on Potentiometry of GaN

J.B. Park[1], T. Niermann[1], M. Beleggia[2], M. Lehmann[1]

[1]TU Berlin, Institut für Optik und Atomare Physik, Berlin, Germany
[2]Technical University of Denmark, Center for Electron Nanoscopy, Kgs. Lyngby, Denmark

park@physik.tu-berlin.de
Keywords: GaN, p-n Junction, off-axis EH

Off-axis electron holography (EH) allows retrieving the phase modulation of the electron wave emerging from a thin sample in the transmission electron microscope. When the sample contains a p-n junction, such phase modulation is determined primarily by the potential difference at thermal equilibrium between the p- and n-regions: the built-in potential V_{pn} [1]. Here we measure the built-in potential of two GaN p-n junctions that differ in their acceptor density (Si-donor concentration: $N_d=2x10^{18}$ cm^{-3}, Mg-acceptor concentration: $N_a=6x10^{19}$ cm^{-3} in sample A and $N_a=2x10^{17}$ cm^{-3} in sample B), and we assess the influence of the electron beam on the measured V_{pn}.

The specimen is prepared by focused ion beam (FIB) at 30 kV by successive reducing the Ga-Ion current. We use the H-bar technique in two perpendicular directions for producing a square-shape needle specimen [2]. No further polishing steps such as Ar-Ion Milling are employed.

In absence of a magnetic field and under kinematic conditions the phase modulation is described by the equation $\varphi = \sigma \cdot V_{GaN} \cdot t_{total} + \sigma \cdot V_{pn} \cdot (t_{total} - t_{dead})$, where σ is an accelerating voltage dependent constant (σ=6.53x10^{6} $V^{-1}m^{-1}$ at 300 kV), V_{GaN} the mean inner potential of GaN, V_{pn} the built-in potential step and t_{total} the sample thickness penetrated by the electrons. The remaining phenomenological parameter, t_{dead} is the "electrically-inactive thickness", describing the effects of amorphous surface layers and the surface depletion layers created by the semiconductor-vacuum interfaces. For the amorphous layer a thickness of (19 ± 7) nm is used, which was determined from previous study. The surface depletion layers depend on the doping concentrations on either side of the junction, and on the position of surface states (if present) within the band gap; for the sake of simplicity, the surface depletion layers are neglected here.

Figure 1 shows the procedure to determine the thickness t_{total}. We measure the length w from a set of unwrapped phase images, each acquired with a different α-tilt angle. The thickness *t* is obtained by a fitting the measured w(α) data set with a sine function, since geometry dictates that $w = t \cdot \sin\alpha$. The thickness t_{total} can then be derived from t_{total} = t/cosα. For our samples we get (t_{total} - t_{dead}) = (416 ± 2) nm for the high p-doped sample A and (t_{total} - t_{dead}) = (397 ± 4) nm for the low p-doped sample B considering the amorphous layers described earlier.

The measurements yield dramatically low built-in potential values in the range of 0.22 V: about 15 times smaller than expected for GaN p-n junction specimens ($V_{pn,A}$= 3.39 V, $V_{pn,B}$= 3.24 V). Expectations are based on the bulk theory of p-n junctions with known doping concentrations [3].

In order to investigate the contribution of illumination to the built-in potential, we varied the electron dose rate while illuminating both specimens, and observed an enhancement of the measured built-in potential by reducing the electron dose rate: the built-in potential increases roughly by 18% in sample A and up to 41% in sample B (Figure 2). We interpret the results as beam-induced generation of electron-hole pairs in sufficient numbers to alter significantly the built-in potential.

Additionally, we observe a markedly different charging character on the specimen by modification of the surface properties, which might be closely connected to the variation of conductivity at the surface. In figure 3(b) the specimen is examined after FIB-preparation. The FIB-preparation produces normally a damaged amorphous surface, which can serve as a conductor. Thus, the effect of the charging with respect to the ground is minute. However, after a change of the surface properties by using the plasma cleaner to remove organic contamination, the stray fields around the specimen has clearly increased (Figure 3(c)). Removing the amorphous surface by wet-etching (KOH) leads to even stronger charging as can be seen from the stray fields (Figure 3(d)).

1. H. Lichte and M. Lehmann, Rep. Prog. Phys. 71 (2008), p. 1.
2. A. Lenk, Dissertation, Dresden (2008).
3. S.M. Sze in “Physics of Semiconductor Devices”, 2., John Wiley & Sons (1981), p.75.
4. This work is carried out as the DFG collaborative research center SFB787 semiconductor nanophotonics

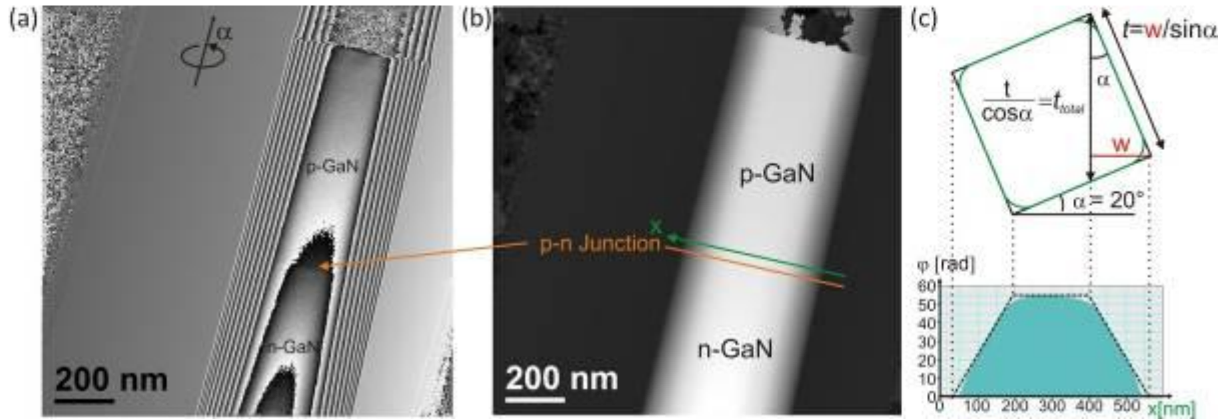

Figure 1. (a) Reconstructed phase of the FIB-prepared square-shape needle at α-tilt angle 20°. The phase variation at the p-n junction is clear visible. (b) Unwrapped phase. The gradually slope is observable at each edge due to the increase of the thickness. (c) Schematic diagram of the expected geometry of the needle with the corresponding profile of the phase along x (green arrow) is depicted.

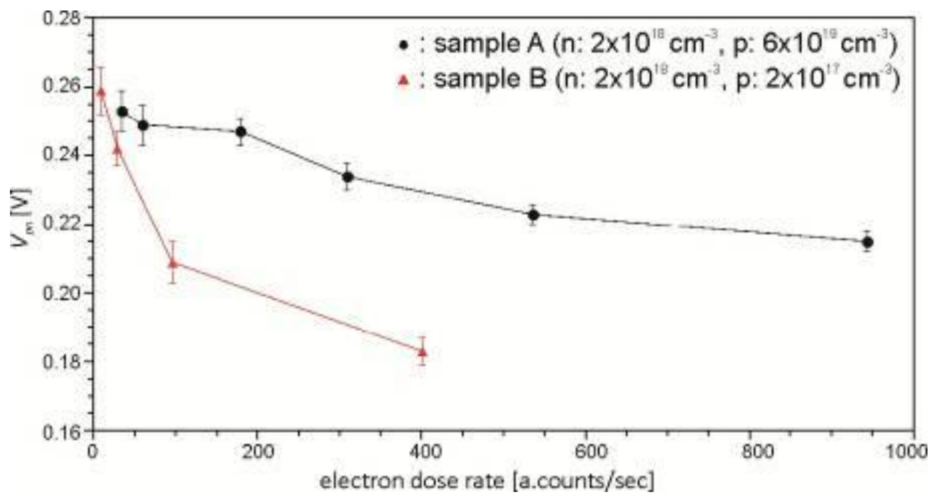

Figure 2. The built-in potential V_{pn} over the electron dose rate is showed from two different GaN p-n junctions, in which the doping concentration of p-GaN is changed.

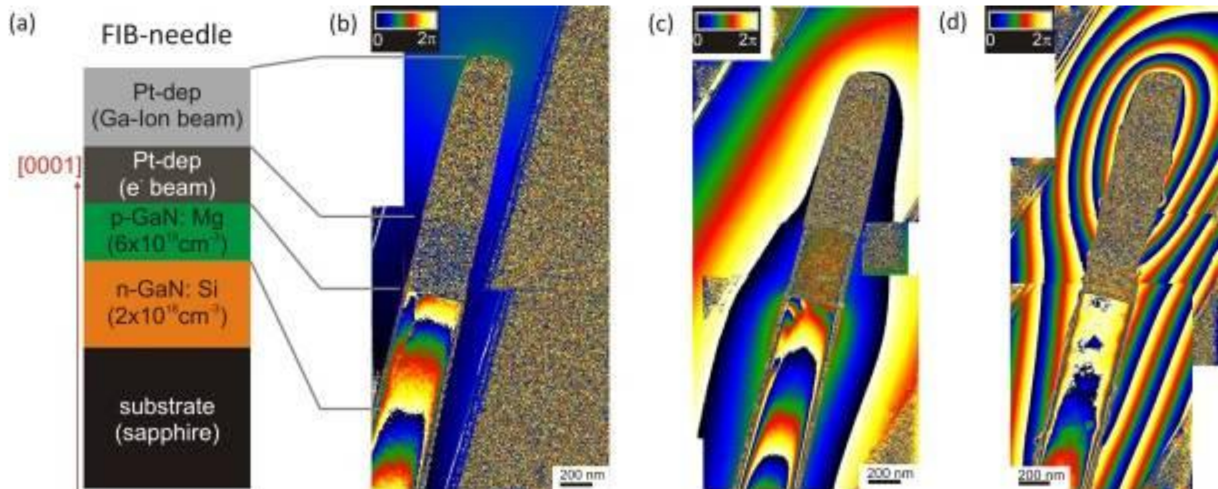

Figure 3. (a) The specimen structure. Each map of the reconstructed phases consists of several reconstructed holograms: (b) The reconstructed phase map of the needle after FIB-preparation. (c) After 5 min plasma cleaning treatment. (d) After 1 min KOH wet-etching.